



Dot Size Dependence of Magnetization Reversal Process in L10-FePt Dot Arrays

著者	高梨 弘毅
journal or publication title	IEEE Transactions on Magnetism
volume	44
number	11
page range	3464-3467
year	2008
URL	http://hdl.handle.net/10097/47221

doi: 10.1109/TMAG.2008.2002503

Dot Size Dependence of Magnetization Reversal Process in L1₀-FePt Dot Arrays

Dongling Wang¹, Takeshi Seki¹, Koki Takanashi¹, Toshiyuki Shima², Guoqing Li³, Hitoshi Saito⁴, and Shunji Ishio⁵

¹Institute for Materials Research, Tohoku University, Sendai 980-8577, Japan

²Faculty of Engineering, Tohoku-gakuin University, Tagajyo 985-8537, Japan

³School of Physics, Southwest University, Chongqing 400715, P. R. China

⁴Faculty of Engineering and Resource Science, Akita University, Akita 010-8502, Japan

⁵Venture Business Laboratory, Akita University, Akita 010-8502, Japan

The dot size dependence of the magnetization reversal process in perpendicularly magnetized L1₀-FePt dot arrays has been investigated in terms of minor loop measurement and magnetic domain observation. For the dots with diameters of 0.25 and 1 μm , the initial applied field ($H_{\text{in}}^{\text{sat}}$) required to saturate the coercivity in the minor loop starting from the thermally demagnetized state is smaller than saturated coercivity (H_c^{sat}), indicating a typical nucleation-type magnetization reversal process. For the dots with diameters of 2.3 and 5 μm , on the other hand, $H_{\text{in}}^{\text{sat}}$ is larger than H_c^{sat} . The magnetic force microscopy images show that the field to wipe out domain walls increases with the dot size, which is consistent with minor loop measurements. The phenomenological analysis for the dots with diameters of 0.25 and 1 μm indicates that irrespective of the dot size the annealing reduces the size of the defect regions and leads to the enhancement of the coercivity due to the recovery from the microfabrication damage.

Index Terms—L1₀-FePt alloy, magnetic domain structure, magnetization reversal process, microfabricated dot arrays.

I. INTRODUCTION

RECENT development of areal density of magnetic recording has already achieved 200 Gbit/in², and is progressing to achieve terabit recording. The demand for ultrahigh density magnetic storage devices drives the bit size into a nanometer scale. However, a crucial issue for nanometer-sized magnetic materials is the thermal instability of magnetization due to the reduction of their magnetic volumes. L1₀-FePt alloy is one of the most promising materials for future ultrahigh density magnetic storage devices because its huge uniaxial magnetocrystalline anisotropy ($K_{\text{u}} = 7 \times 10^7$ erg/cc) [1] leads to the excellent thermal stability of magnetization.

Self-assembled FePt particulate films and lithographically patterned FePt dot arrays showed nucleation-type magnetization reversal processes [2], [3], and their coercivities (H_c) depended strongly on the film morphology and the dot size. The understanding of the detailed mechanism on magnetization reversal processes is important for practical application. A phenomenological analysis, proposed by Kronmüller and his collaborators [4], [5], described the magnetization reversal process of sintered permanent magnets such as Nd-Fe-B and Sm-Co from the viewpoint of the inhomogeneity of microstructure, and has been applied to a wide range of magnets [6], [7]. The phenomenological analysis enables us to evaluate the defect region for the nucleation of a reversed domain. In a previous paper [8], the phenomenological analysis was applied to microfabricated FePt dots with a diameter of 0.25 μm , and its result showed that the defect region phenomenologically analyzed was reduced by post-annealing, which led to the increase of H_c [8]. This implies that the size of the defect region is related with H_c .

This paper reports the dot size dependence of the magnetization reversal process for FePt dot arrays with different dot sizes. Their initial magnetization reversal processes have been investigated in terms of minor loop measurement and magnetic domain observation. Furthermore, the dot size dependence of H_c , the defect region ($2r_0$), and the effective demagnetizing factor (N_{eff}) are discussed based on the phenomenological analysis.

II. EXPERIMENTAL PROCEDURE

A thin film with the layered structure of FePt (50)/Au (40)/Fe (1) (in nanometers) was first prepared on a MgO (001) single-crystal substrate using an ultra-high voltage (UHV) compatible magnetron sputtering system. Fe seed and Au buffer layers were deposited at room temperature, and a FePt layer was epitaxially grown at 300 °C, and subsequently annealed at 500 °C for 15 min. FePt dots with a circular shape were fabricated through the use of electron-beam lithography and Ar ion etching. The microfabrication process was the same as that used in previous studies [3], [8]. The diameter of the dot (d) was varied in the range from 0.25 to 5 μm . Post-annealing after microfabrication was performed at 500 °C for 15 min. The structure was characterized by X-ray diffraction, which confirms that the epitaxial layered structure is not changed even after microfabrication, and the preferential crystallographic orientation of the FePt layer is the [001] direction. The magnetization curves of FePt dots were measured in the temperature range from 50 to 310 K using a superconducting quantum interference device (SQUID) magnetometer. The magnetic domain structure was observed at room temperature by a magnetic force microscopy (MFM), which was performed with applied field in the range from 0 to 5 kOe.

III. EXPERIMENTAL RESULTS AND DISCUSSION

The magnetization curves for an unpatterned continuous film and the dot array with $d = 0.25$ μm are shown in Fig. 1. The solid curve represents the result of the dot array, and the broken

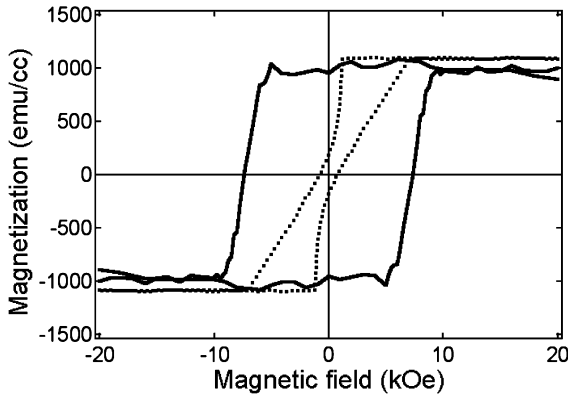


Fig. 1. Magnetization curves for a continuous film (broken line) and FePt dots with the diameter of $0.25\ \mu\text{m}$ (solid line). The magnetic field was applied in the perpendicular direction to the film plane.

one represents that of the continuous film. The magnetic field was applied perpendicularly to the film plane. For both cases, the easy magnetization axes are the perpendicular direction to the film plane. The continuous film shows small H_c of 0.8 kOe. After patterning the continuous film into the dot shape, H_c drastically increases up to 7.5 kOe. The dots with other diameters also show the increase of H_c after patterning as shown later.

In order to investigate the initial magnetization reversal process, the minor hysteresis loops were measured. Fig. 2(a) shows the minor hysteresis loop for the FePt dots with $d = 5\ \mu\text{m}$ after applying an initial field (H_{in}) of 5 kOe. The sequence of the measurement was denoted by the arrows. Starting from the thermally demagnetized state, magnetic field is increased up to H_{in} , and then reversed to $-50\ \text{kOe}$. Finally, the full hysteresis loop was measured from $-50\ \text{kOe}$ to $+50\ \text{kOe}$. The value of H_c , which is the coercive field in the negative field region for the minor hysteresis loop, is obtained to be 0.6 kOe for the dots with $5\ \mu\text{m}$ at $H_{in} = 5\ \text{kOe}$. Through the same sequence, the minor hysteresis loops were measured with different H_{in} for all the dot arrays. The results were summarized as the H_{in} dependence of H_c of the minor hysteresis loops in Fig. 2(b). For $d = 0.25$ and $1\ \mu\text{m}$, the fields to saturate H_c in minor loops (H_{in}^{sat}) are significantly smaller than the saturated values of $H_c(H_c^{\text{sat}})$, which indicates a nucleation-type magnetization reversal process. For $d = 2.3$ and $5\ \mu\text{m}$, however, the values of H_{in}^{sat} are larger than H_c^{sat} . It is obvious that H_c^{sat} increases with decreasing d . In Fig. 2(c), H_c and H_{in} were normalized by H_c^{sat} , where H_c^{sat} corresponds to H_c of the full hysteresis loop. For $d = 0.25$ and $1\ \mu\text{m}$, $H_{in}^{\text{sat}}/H_c^{\text{sat}} < 1$, while for $d = 2.3$ and $5\ \mu\text{m}$, $H_{in}^{\text{sat}}/H_c^{\text{sat}} > 1$, which indicates that the initial magnetization process does not show typical nucleation-type behavior in the case of the dots with larger diameters. Fig. 3 shows MFM images for the dots with $d = 0.25\ \mu\text{m}$ (Fig. 3(a)–(d)) and $1\ \mu\text{m}$ (Fig. 3(e)–(h)) when the applied magnetic field is increased from 0 to 5 kOe gradually. In the initial state ($H_{in} = 0\ \text{kOe}$), multiple domains are observed for both diameters, where the bright and dark contrasts correspond to the magnetization directions upward and downward, respectively. Compared with the result for $d = 0.25\ \mu\text{m}$ including three or four domains, the dots with $d = 1\ \mu\text{m}$ have a large number of domains. When a

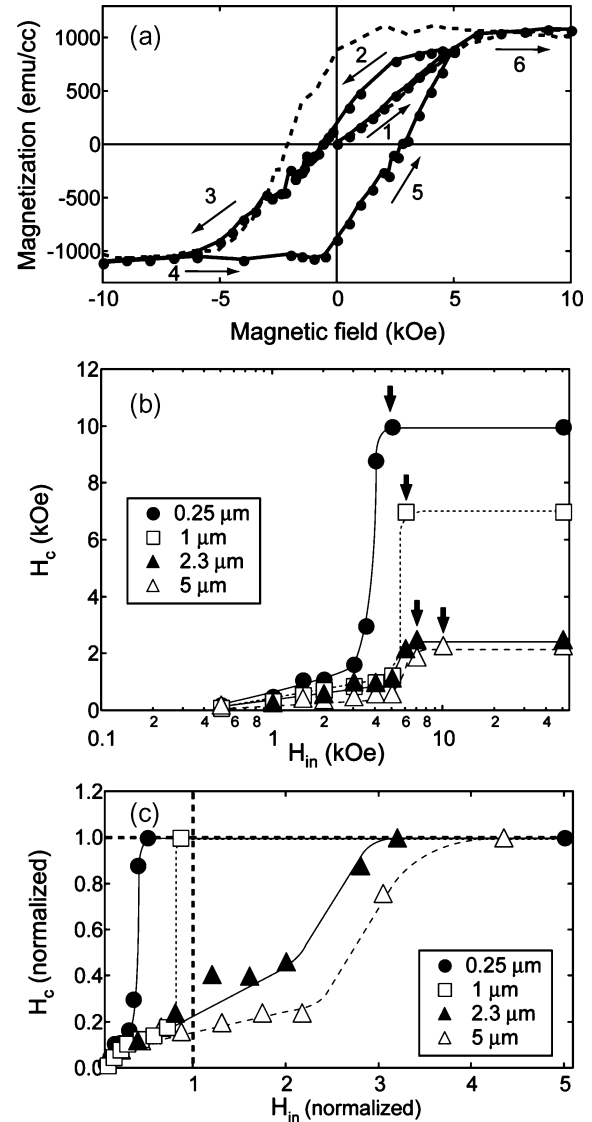


Fig. 2. (a) Minor hysteresis loop (solid circles) for the dots with the diameter of $5\ \mu\text{m}$. The initial magnetic field (H_{in}) of 5 kOe was applied. The arrows denote the sequence of the measurement. The broken line is the full hysteresis loop. (b) H_{in} dependence of the coercive field in the minor hysteresis loop (H_c) for FePt dots with the diameters of $0.25\ \mu\text{m}$ (solid circles), $1\ \mu\text{m}$ (open squares), $2.3\ \mu\text{m}$ (solid triangles), and $5\ \mu\text{m}$ (open triangles). (c) H_c normalized by the coercivity of the full hysteresis loop (H_c/H_c^{sat}) as a function of H_{in} normalized by the same value of coercivity (H_{in}/H_c^{sat}).

magnetic field of 2 kOe is applied, the bright region expands and the dark region shrinks, which means the movement of domain walls. With increasing the magnetic field to 5 kOe, the expansion of the bright region is more obvious for $d = 0.25\ \mu\text{m}$, and the dots with $d = 0.25\ \mu\text{m}$ entirely turns bright. In other words, the multiple-domain state changes into the single-domain state. For $d = 1\ \mu\text{m}$, however, the domain walls still remain in the dots. Comparing the result for $d = 0.25\ \mu\text{m}$ with that for $d = 1\ \mu\text{m}$, the domain walls for $d = 0.25\ \mu\text{m}$ are easily wiped out by small initial magnetic field. These results imply that the multiple-domain state becomes stable with increasing d . The increase of the dot size corresponds to the increase of the aspect ratio of the diameter to the height of the dot. Therefore,

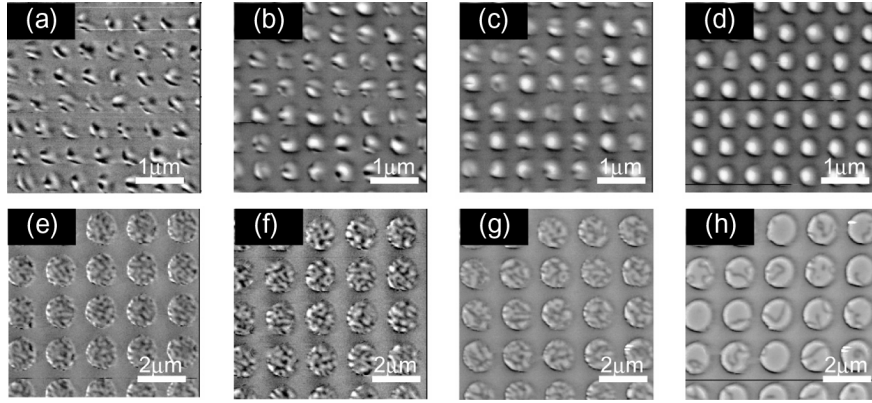


Fig. 3. MFM images for the FePt dots with the diameters of $0.25 \mu\text{m}$ ((a)–(d)) and $1 \mu\text{m}$ ((e)–(h)). The MFM observation was performed at the magnetic field of 0 kOe ((a) and (e)), 2 kOe ((b) and (f)), 3 kOe ((c) and (g)), and 5 kOe ((d) and (h)).

TABLE I
 H_c , M_s , K_u , α , $2r_0$, AND N_{eff} FOR DOTS WITH $d = 0.25$ AND $1 \mu\text{m}$ BEFORE AND AFTER ANNEALING

	0.25 μm		1 μm	
	Before annealing	After annealing	Before annealing	After annealing
H_c (kOe)	7.5	10	6	7
M_s (emu/cm ³)	1020	1060	978	1015
K_u (erg/cm ³)	2.5×10^7	3.0×10^7	3.0×10^7	3.2×10^7
α	0.13	0.19	0.1	0.21
$2r_0$ (nm)	26 (± 1)	18 (± 2)	34 (± 13)	13 (± 3)
N_{eff}	$4\pi(-0.05 \pm 0.02)$	$4\pi(0.12 \pm 0.09)$	$4\pi(0.00 \pm 0.30)$	$4\pi(0.52 \pm 0.20)$

the magnetostatic energy in the single domain state increases with d , which leads to the stable multiple-domain state.

The phenomenological analysis of the magnetization reversal process allows us to evaluate $2r_0$ and N_{eff} for the FePt dots. Taking into account the deviation of a real magnet from the ideal situation, the phenomenological analysis modifies H_c from the theoretical limit, and it is given by

$$H_c = \alpha \frac{2K_u}{M_s} - N_{\text{eff}} M_s \quad (1)$$

where K_u and M_s are uniaxial magnetic anisotropy and saturation magnetization, respectively, and two microstructural parameters α and N_{eff} are introduced. N_{eff} is an averaged local effective demagnetization factor. α includes the pinning or nucleation effect of the inhomogeneity of magnetocrystalline energy (α_K) and the effect of the misalignment of grains (α_ψ). Then, $\alpha = \alpha_K \alpha_\psi$. From the X-ray diffraction pattern (not shown here), α_ψ was obtained to be 0.95. α_K is given by $\alpha_K = \delta_B / \pi r_0$, where δ_B is the domain wall width of ~ 5.7 nm. Consequently, the value of α is related with $2r_0$. The parameter fitting of the temperature dependence of H_c , K_u , and M_s to the formula (1) gives α and N_{eff} (detailed procedure has been published elsewhere [8]). As we discussed above, the minor loops for $d = 0.25$ and $1 \mu\text{m}$ show typical nucleation-type behavior. Then, the phenomenological analysis was applied to those dot arrays. Table I summarizes H_c , M_s , K_u , α , $2r_0$, and N_{eff} for the dots with $d = 0.25$ and $1 \mu\text{m}$ before and after annealing. For both dots with $d = 0.25$ and $1 \mu\text{m}$, H_c increases and $2r_0$ is reduced after annealing, which supports that the value of $2r_0$ is an important parameter to determine H_c . The

present relationship between $2r_0$ and H_c is consistent with the results reported previously [8], which indicates the annealing promotes the recovery from damages, leading to the reduction of $2r_0$ and the enhancement of H_c . Although $2r_0$ is reduced and H_c increases irrespective of the dot size, which supports that the increase of H_c results from the reduction of $2r_0$ by annealing, there is no clear correlation between the dot size and $2r_0$ observed in the present result, and further systematic investigation will be required to elucidate this point. Both the dot arrays show small N_{eff} compared with those for sintered permanent magnets. These small N_{eff} may result from the high crystallinity of epitaxial films and/or the small dipolar interaction between dots with well-defined geometry prepared by lithographical technique.

Although the initial magnetization processes for $d = 2.3$ and $5 \mu\text{m}$ seem to show not typical nucleation-type behavior but rather pinning-type behavior as shown in Fig. 2(c), the pinning-type reversal does not explain its magnetization reversal process. Note the full magnetization curves for $d = 5 \mu\text{m}$ shown in Fig. 2(a). The nucleation of the reversed domains easily occurs at a low magnetic field and the reversed domains smoothly propagate. If the domain wall pinning is the main magnetization reversal process, the reversed domains are trapped by pinning sites and H_c may show a larger value. Therefore, we consider the magnetization reversal processes for $d = 2.3$ and $5 \mu\text{m}$ are a kind of nucleation-type reversal process as in the case of $d = 0.25$ and $1 \mu\text{m}$. However, the stability of the multiple-domain state strongly depends on the dot size, which determines the required magnetic field to wipe out the domain walls from the dot.

IV. CONCLUSION

The magnetization reversal process was investigated for the FePt dots with different d . Initial magnetization process for dots with $d = 0.25$ and $1\ \mu\text{m}$ showed typical nucleation-type behavior. For $d = 2.3$ and $5\ \mu\text{m}$, however, the larger $H_{\text{in}}(> H_{\text{c}}^{\text{sat}})$ was required to wipe out the domain walls due to the increase of the magnetostatic energy. The phenomenological analysis for $d = 0.25$ and $1\ \mu\text{m}$ shows annealing promotes the recovery from the damage, which leads to the reduction of $2r_0$ and the enhancement of H_{c} . All the dot arrays showed small N_{eff} compared with those for sintered permanent magnets.

ACKNOWLEDGMENT

This work was supported in part by the Global COE Program "Materials Integration," Tohoku University. The microfabrication was partly performed at the Advanced Research Center of Metallic Glasses, IMR, Tohoku University.

REFERENCES

- [1] O. A. Ovanov, L. V. Solina, V. A. Demshina, and L. M. Magat, "Determination of the anisotropy constant and saturation magnetization, and magnetic properties of powders of an iron-platinum alloy," *Phys. Met. Metallogr.*, vol. 35, pp. 81–85, 1973.
- [2] T. Shima, K. Takanashi, Y. K. Takahashi, K. Hono, G. Q. Li, and S. Ishio, "Nucleation-type behavior of magnetization in FePt (001) particulate films," *J. Appl. Phys.*, vol. 99, pp. 0335161–0335165, 2006.
- [3] T. Seki, T. Shima, K. Yakushiji, K. Takanashi, G. Q. Li, and S. Ishio, "Dot size dependence of magnetic properties in microfabricated L1₀-FePt (001) and L1₀-FePt (110) dot arrays," *J. Appl. Phys.*, vol. 100, pp. 0439151–0439158, 2006.
- [4] H. Kronmüller, "Micromagnetism in hard magnetic materials," *J. Magn. Magn. Mater.*, vol. 7, pp. 341–350, 1978.
- [5] H. Kronmüller, K.-D. Dust, and M. Sagawa, "Analysis of the magnetic hardening mechanism in Re-FeB permanent magnets," *J. Magn. Magn. Mater.*, vol. 74, pp. 291–302, 1988.
- [6] R. Skomski, "Exact nucleation modes in arrays of magnetic particles," *J. Appl. Phys.*, vol. 91, pp. 7053–7055, 2002.
- [7] R. Skomski, "Nanomagnetics," *J. Phys.: Condens. Matter.*, vol. 15, pp. R841–R896, 2003.
- [8] D. Wang, T. Seki, K. Takanashi, and T. Shima, "Magnetization reversal process in microfabrication L1₀-FePt dots," *J. Appl. Phys. D: Appl. Phys.*, vol. 41, pp. 1950081–1950086, 2008.

Manuscript received March 03, 2008. Current version published December 17, 2008. Corresponding author: K. Takanashi (e-mail: koki@imr.tohoku.ac.jp).